

AN OPTIMIZED MRI-BASED BRAIN TUMOR SEGMENTATION: A COMPARATIVE STUDY OF IMPROVED CLUSTERING MECHANISMS

Mohit Prakram, Kirti Rawal, Manu Prakram and Parul Sharma

MSC 2010 Classifications: Primary 33C20, ; Secondary 33C65

Keywords and phrases: Comparative models, Cancer, Brain Tumour, Traditional segmentation, Clustering, Fuzzy C-means, K-means, Particle Swarm Optimization, Moth Flame Optimization and MRI.

The authors would like to thank the reviewers and editor for their constructive comments and valuable suggestions that improved the quality of our paper.

Abstract

An accumulation or abnormal multiplication of brain cells is called a brain tumor, which can be benign or malignant. Anatomical site, cellular composition, and primary or secondary status classify brain tumours, but early detection is crucial for enhancing treatment efficacy, enhancing patient prognosis, and lowering health risks. In this research article, a comparative analysis is performed based on the traditional as well as clustering-based approaches with Meta heuristic methods to improve the Region of Tumor segmentation (ROT). Basically, we proposed six different scenarios such as Fuzzy C-means (FCM) based, K-means-based, FCM with Particle Swarm Optimization (PSO) based, K-means with PSO-based, FCM with Moth Flame Optimization (MFO) based, K-means with MFO-based segmentation. To solve the clustering-based segmentation problem, optimisation techniques are used with a novel fitness function that helps to minimise the pixel mixing problem and helps to improve the segmentation quality and return better ROT. We use a publicly available and standard dataset, the MRI Benchmark Dataset, which includes both cancerous and non-cancerous data, to perform model simulation and calculate the performance parameters. The suggested system using the K-means algorithm with the MFO has better segmentation accuracy than other approaches and previous works, according to experiments. Most MRI sample photos exceed 99%. A model that combines K-means and MFO as an optimisation technique separates the ROT from a human brain MRI image in seconds. Therefore, this combination is best for tumor classification using accurate segmented ROT with the highest efficiency.

1 Introduction

The growth of a brain tumor may result from an excessive number of aberrant cells in the human body [1]. We can broadly classify the growth of tumours in the human body into two categories: benign and malignant [2]. We now recognise that a combination of genetic, molecular, and conservational issues influences brain tumours, underscoring their intricate relationship [3]. As these proliferating aberrant cells expand without restraint, they can disturb the typical operation of the brain, leading to a variety of health complications [4]. Progress in medical science and technology has facilitated a more detailed understanding of the processes involved in tumour development [32], allowing for novel strategies in the areas of diagnosis, therapy, and control. Figure 1 depicts a description of both types of tumours. The brain is a complicated organ in the human body with 50–100 billion neurons. Each of its many cells has a specific function to perform a specific task. For proper body function, most body cells divide to make new cells, and the older, damaged cells die when new ones grow [5]. Sometimes the body produces unnecessary cells, and additionally, injured or old cells do not die properly. Tumours form from excess

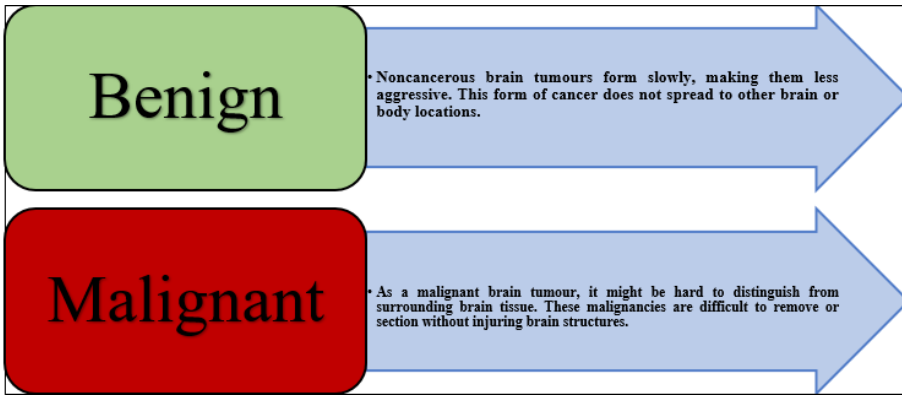


Figure 1. Types of Human Brain Tumour

cells in the body, and brain tumours alter sensitive body functions. Treatment is dangerous because of its location and spread [6, 7, 8]. The two main forms of brain tumours are benign and malignant, according to Figure 1. Figure 2A depicts a healthy brain image, while Figure 2B displays a cancerous brain image, making the distinction between the two types of brain tumors clear [9]. Researchers use Computer-Aided Design (CAD) systems for analytical and specific brain disorder detection [10]. Abnormal tissue or central spine growths, known as brain tumours, disrupt brain function [11]. The National Cancer Institute Statistics (NCIS) conducted a survey that revealed 12,764 brain cancer deaths annually, 1063 monthly, 245 weeklies, and 34 daily in the US alone, indicating a significant global impact. In order to preserve lives, advanced brain tumour diagnosis is crucial, requiring fast and accurate tumour detection. This can only be achieved through the use of magnetic resonance imaging (MRI) scans, which segment complex medical images to extract questionable regions. There are lots of imaging techniques, such as CT, PET scans, and angiography, available, but MRI is more accurate. So, this study underscores the significance of MRI scan data in refining and advancing current segmentation methodologies [12].

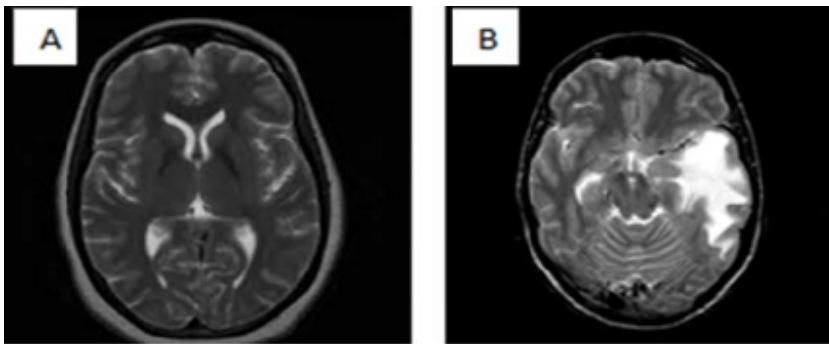


Figure 2. A. Healthy Brain and B. Cancerous Brain

Motivation

According to the study, detection of tumour at an early stage is a beneficial way to protect human lives, and the motivation behind undertaking this study is rooted in the critical need for advancements in medical imaging technology to enhance the diagnosis and treatment of brain tumours. Brain tumors pose significant healthcare challenges due to their complexity and diverse characteristics, which necessitate precise and efficient segmentation techniques for accurate analysis. Current medical research has made remarkable strides in understanding brain tumors, and MRI has become a cornerstone in their detection. Nevertheless, the process of dividing these tumours into segments continues to be a difficult undertaking, frequently susceptible to mistakes and imprecisions. The motivation behind this study is to address these challenges head-on by exploring

and comparing improved clustering mechanisms by utilising the concept of swarm-based approaches such as Particle Swarm Optimization or Meta heuristics (PSO), Artificial Bee Colony (ABC), Firefly Algorithm (FFA), Cuckoo Search Algorithm (CSA), and Moth-Flame Optimization (MFO) as shown in Figure 3 [13].

Contribution

By conducting a comparative analysis of existing segmentation approaches, this research aims to identify and optimize clustering mechanisms that can significantly enhance the accuracy and efficiency of MRI-based brain tumor segmentation [43]. The potential impact of this optimization extends beyond research laboratories and into clinical settings, offering healthcare professionals a more reliable tool for early detection and diagnosis of tumours. The quest for an optimised segmentation technique is not merely an academic pursuit; it is a mission to improve patient outcomes and contribute to the ongoing evolution of medical practices. Through this study, we aspire to provide valuable insights that can revolutionise the way we approach brain tumor analysis, fostering advancements that hold the promise of more accurate diagnoses, timely interventions, and ultimately improved patient care. In a world where medical innovation is paramount, this research seeks to be a catalyst for positive change in the realm of neuroimaging and brain tumor diagnostics. The major contributions are listed as:

1. We present a short survey on detection and segmentation of brain tumour to identify the challenges and issues.
2. Pre-processing methods are employed to enhance the quality of MRI data and improve the clarity of images.
3. To detect and segment the Region of Tumour (ROT) from MRI data, a comparative analysis is performed for FCM and K-means with swarm-based optimization method that is presented in the Figure 4.
4. To validate and find out best tactic, performance parameters is calculated and compared in terms of Sensitivity, Precision, F1-score, Mathew Correlation Coefficient (MCC), Dice, Jaccard, Specificity, Accuracy, and Time.

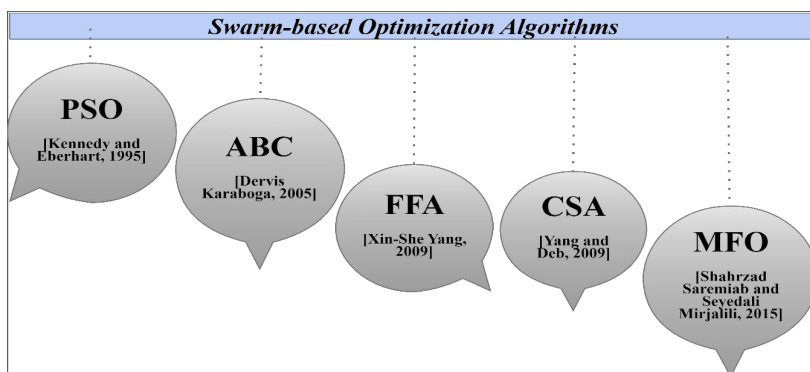


Figure 3. Latest Swarm-based Algorithms

The proposed comparative model's block strategy is depicted in Figure 4. Essentially, we describe a comparative brain tumour segmentation model using clustering-based methods and their hybridization with swarm-based optimisation approaches to improve the efficiency of segmentation techniques. In this study, two distinct scenarios—one using the hybridization of K-means with PSO and MFO and the other involving the hybridization of FCM with PSO and MFO. This section of the research paper presents an introduction to the fundamental concept of brain tumour segmentation using MRI scans. The subsequent sections are structured as follows: The literature review on brain tumour segmentation using MRI images is described in Section 2. The methodology and resources used for the comparative study are explained in Section 3, while the findings and comments are presented in Section 4. The research's general conclusion is outlined in Section 5, discussing potential future advancements in automatic brain tumour segmentation.

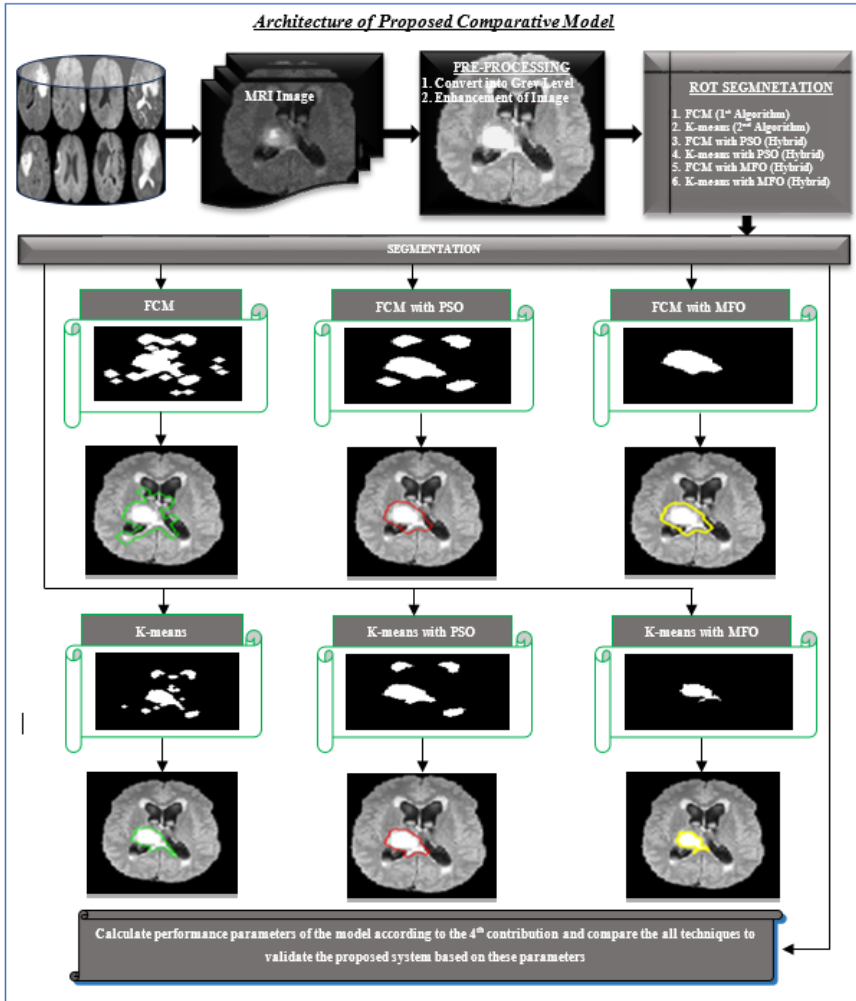


Figure 4. Architecture of Proposed Comparative Model

1.1 Contextual Review

In exploring into the landscape of brain tumor segmentation, a comprehensive literature survey lays the foundation for understanding the evolving methodologies and technological advancements in this critical domain. Examining prior studies provides valuable insights into the challenges and breakthroughs, shaping the context for our novel approach in this article. So, we present an overview of the most significant prior related to the clustering-based with swarm approach for medical image segmentation techniques. Firstly, in 2011, **Chander et al.** had published an article related to the image segmentation using the concept of Otsu's method by modifying it through the swarm-based PSO approach in Elsevier. In this study, the authors utilized the notion of Particle Swarm Optimization (PSO) to improve the performance of Otsu's technique for picture segmentation. The effectiveness of this enhancement was evaluated through experimental analysis. Furthermore, it was demonstrated that the enhanced segmentation method surpassed other established methodologies [13]. **Bandyopadhyay and Paul** then developed a K-means clustering-based diagnosis system to segment brain tumours from MRI images in 2013. To improve brain tumour segmentation, the authors split the algorithm into two steps. The first involved picture registration, and the second involved MRI image fusion. After that, they use enhanced K-means to segment MRI tumours. The design system was limited by the data pattern and unsuitable for 3D medical picture segmentation modelling due to segmentation mixing [14]. **Zhao et al.** in 2014 developed a model to handle the pixel mixing problem using the concept of K-means clustering-based medical image segmentation. The PSO is introduced here to improve K-means tumour segmentation using MRI. The PSO principle is used to form initial clusters for MRI data based on their pixels, and then fitness is applied to address the issue of mixing. In experiments, PSO-based modified K-means outperformed normal K-means in accuracy and execution time for the segmentation of medical images mostly for brain tumor data [15]. In the same year, IJIRCCE released a brain tumour segmentation study using classical Fuzzy C-means (FCM). Additionally, sophisticated K-means was employed to locate tumour areas from MRI [16, 27]. **Parasar and Rathod** compared seeded region growth, watershed, and FCM with swarm-based PSO for ultrasound image segmentation using PSO and K-means in 2017 [17]. **Ventateshan and Parthiban** created an MRI image segmentation algorithm in 2017 by hybridising fuzzy K-means with PSO and kernel-based fuzzy K-means. The technique was evaluated for its faster execution time; however, accuracy needs improvement [18].]. In 2017, **Yuan et al.** performed skin lesion segmentation using deep fully CNN using Jaccard distance [29]. Experimental results showed that the proposed method outperformed other state of art algorithms. In 2018, **Riaz et al.** used Active contours-based segmentation and lesion periphery analysis for characterization of skin lesions in dermoscopy images [30]. The proposed method outperformed other methods that have been used for comparison. **Hasan** used PSO as a swarm intelligence approach to segment brain tumours from MRI data in 2018. With contour-based segmentation and PSO, they achieved 92% segmentation accuracy [19]. **Karegowda et al.** studied MRI tumour segmentation in 2018. After comparing K-means, FCM, PSO, and Adaptive Regularised Kernel-based FCM (ARK-PSO), they determined that PSO is a good swarm intelligence approach. In experiments, PSO-based segmentation outperformed K-means, FCM, and Adaptive Regularised Kernel FCM [20]. Using K-means, **Arun Kumar et al.** improved brain tumour segmentation and identification automation in 2019. To properly predict a brain tumour, the authors enhanced the picture during pre-processing [21]. In 2019, **Blousselham et al.** studied brain tumor segmentation on MRI images based on temperature changes on pathologic area [28]. The obtained results in all patients showed significant improvement using the proposed method. In 2019, **Vasconcelas et al.** performed Automatic skin lesions segmentation based on a new morphological approach via geodesic active contour [31]. The results proved that the method can be effectively used for skin lesion segmentation. In same year two more studies on skin lesion segmentation were performed by **Sullivan et al.** [33] and **Wei et al.** [34]. **Tan et al.** used enhanced particle swarm optimization for image segmentation in 2019 [35]. In 2020, **Xie et al.** performed Skin lesion segmentation using high-resolution convolutional neural network. The proposed network could accurately extract skin lesion boundaries and was robust to artefacts in the images [36]. Some more studies in context to blood cancer detection using leukaemia image segmentation related to the work have been studied [37, 38, 39, 40, 41, 42]. In these studies also Fuzzy C mean (FCM) or k means clustering algorithm has been used for white blood cell

segmentation. *Hrosik et al.* hybridised K-means with FFO to improve segmentation precision for Harvard Whole Brain Atlas brain MRI datasets the same year. Data showed that the hybrid strategy performed best [22]. Chander et al. used K-means and SVM as ML to segment tumours from MRI images in 2020, improving system accuracy [23]. In 2021, *T Magadza and S Viriri* conducted a small survey on brain tumour segmentation using DL plan. This article describes cutting-edge deep learning methods for brain tumour segmentation and their fundamentals. It contains a thorough analysis of medical image processing challenges cite24. In 2021, *Hanuman et al.* proposed a hybrid FCM-PSO algorithm on triangular and real brain datasets and results produced a significant improvement [25]. *K. Anita Davamani et al.* in 2022 Performed accurate cell segmentation through A-FCM clustering with BS-MFO (Best Search based-MFO) which showed improved results [26]. We found the following inferences after reviewing brain tumour region segmentation and detection research:

- Explore medical image segmentation clustering algorithm robustness research gaps. Compare algorithms under different imaging settings like resolution, noise, and picture artefacts.
- Find holes in medical image segmentation clustering algorithm scalability literature. Assess their efficiency and accuracy on huge datasets, taking computational complexity and resource constraints into account.
- Find ways to fix class imbalance in clustering-based medical image segmentation. Assess the influence of uneven class distributions on segmentation performance and suggest bias-reduction strategies.
- Existing pre-processing methods cannot improve normalised MRI images for cancer region segmentation, leading to a high false point rate. The reduced contrast strategy can improve image quality for certain issues.
- Clustering-based segmentation alone is insufficient for medical MRI image segmentation for brain tumour classification.
- In many cases, unsupervised clustering methods like K-means FCM are utilised, resulting in suboptimal segmentation of grey-level MRI.

Based on the above literacy survey, we conclude several essential points about brain tumour segmentation from MRI images, which helps shorten current problems in suggested comparative analysis-based research article. ROT segmentation is a fully automated hybrid method for brain tumour region segmentation with the help of various meta-heuristic algorithms with two famous clustering algorithms named as K-means and FCM. We start with six scenarios all are named as FCM-based (1^{st}), K-means-based (2^{nd}), FCM with PSO-based (3^{rd}), K-means with PSO-based (4^{th}), FCM with MFO-based (5^{th}), K-means with MFO-based (6^{th}) segmentation and compare them in the next portion of this study.

2 Model Methodology

This section of the article describes the proposed comparative system for brain tumour segmentation from MRI data using different approaches and their hybridization. In this research, we compare classic and enhanced segmentation methods for ROT segmentation from brain MRI data. We introduced a comparative scheme using six scenarios:

FCM-based ROT Segmentation:

This suggested system uses FCM for unsupervised clustering-based segmentation of ROT from MRI data. FCM assigns each image pixel to numerous clusters with varying degrees of membership for soft assignments. This soft assignment allows brain tumour segmentation to better depict tissue invariance properties by reflecting medical picture uncertainty and ambiguity [46]. Based on this architecture, FCM creates two parts of an MRI picture: a background and a foreground component, which is the ROT because FCM's capacity to detect tiny gradients and pixel

brightness helps it define tumour boundaries. This helps clinician's plan and track treatment by accurately localising and delineating tumour locations. We apply some pre-processing stages in all six scenarios, starting with MRI image like colour conversion (if needed) using equation 1 and image quality enhancement using algorithm 1 with the help of equation 3.2 and 3.3.

$$\text{MRI}_{\text{Grey image}} = 0.299 \times I(:, :, 1) + 0.587 \times I(:, :, 2) + 0.114 \times I(:, :, 3) \quad (2.1)$$

where $\text{MRI}_{\text{Grey image}}$ is the greyscale MRI image obtained after conversion based on the clipped region of the MRI image for quality enhancement. In this context, $I(:, :, 1)$, $I(:, :, 2)$, and $I(:, :, 3)$ represent the red, green, and blue components of the image, respectively.

Finally, to calculate the average number of pixels in the MRI image, which aids in improving image quality and makes the tumor region more visible, we use the following equation:

$$P_{\text{AVG}} = \frac{P_{(\text{region-x_axis})} \times P_{(\text{region-y_axis})}}{\text{MRI}_{\text{Grey image}}} \quad (2.2)$$

Equation (3.2) determines the average pixel value for the MRI image, where $P_{(\text{region-x_axis})}$ and $P_{(\text{region-y_axis})}$ represent the number of image pixels along the x-axis and y-axis, respectively, in the clipped region of the image (P_{CLIP}).

The clip limit (P_{CL}) for MRI image enhancement is computed using Equation (3.3), after which the procedure is applied to enhance the image.

MRI Enhancement

Input: MRI Images \rightarrow MRI

Output: Enhanced Data of MRI \rightarrow EMRI

1. Start MRI Enhancement
2. Load the MRI
3. Calculate size of MRI-Image = [Row, Col., and D]
4. Set clip limit, $P_{\text{CL}} = P_{\text{CLIP}} - P_{\text{AVERAGE}}$
5. If $D > 1$ then
 - MRI_R = Red Part of MRI
 - MRI_G = Green Part of MRI
 - MRI_B = Blue Part of MRI
 - For I according to Clip Limit do
 - R = Intensity (MRI_R, P_{CL})
 - G = Intensity (MRI_G, P_{CL})
 - B = Intensity (MRI_B, P_{CL})
 - End – For
 - EMRI Image = cat(3, Red, Green, Blue)
 - Else
 - For I according to Clip Limit do
 - EMRI = Intensity (MRI(I), P_{CL})
 - End – For
 - End – If
6. Return: EMRI as an Enhanced MRI image
7. End – Algorithm

We segregate brain tumours from MRI images as foregrounds after MRI enhancement process. It contains tumour pixels and excess pixels from the split part's background. The suggested system with FCM algorithm is:

FCM-based Segmentation

Input: Enhanced Data of MRI → EMRI

Output: Background and Foreground of MRI in terms of ROT → B-MRI and ROT

1. Start FCM-based Segmentation
2. Initialize a group for segmentation ($G = 2$)
3. EMRI Size = [Row, Col, Plane]
4. A predetermined number of clusters, $C = C1$ and $C2$ // Where $C1$ for B-MRI and $C2$ for ROT
5. ITR = N is set for iterations.

6. While ITR \neq N (if maximum iteration is not achieved) do

For m according to Row do

For n according to Col do

If M-Image[m, n] == $C1$ then

B-MRI[m, n] = EMRI[m, n]

Else Default == $C2$

ROT[m, n] = EMRI[m, n]

End – If

End – For

End – For

7. Adjust Centroid C during segmentation using given equation

$$C_{mn} = \frac{\sum_{g=1}^n \gamma_G^m \cdot x_G}{\sum_{g=1}^n \gamma_G^m}$$

8. Repeat and define membership function using given equation

$$[C1, C2] = \sum_{g=1}^n \left(\frac{d_{Gm}^2}{d_{Gn}^2} \right)^{\frac{1}{m-1}}$$

9. End – While

10. Return: B-MRI and ROT as a segmented MRI background and foreground

11. End – Algorithm

For the FCM-based segmentation, we use this technique to segment the ROT from MRI images.

K-means-based ROT Segmentation: In the second scenario of the suggested model, we employed K-means instead of FCM because it yields superior segmentation results. K-means can segment more appropriate tumour regions from MRI scans, but poor contrast images can cause mix-ups, so it cannot always produce better segmentation results. Since it is an unsupervised clustering method, it can divide input MRI image pixels into numerous clusters based on pixel intensity levels. Large datasets and real-time applications benefit from K-means' computational efficiency over Fuzzy C-means. K-means simplicity permits faster convergence, which is important in clinical settings where speedy decision-making is needed. K-means creates clusters with well-defined borders, improving segmentation interpretation. This trait is useful for clinical decision-making when tumour and healthy tissue must be distinguished. The suggested algorithm for K-means-based ROT segmentation is written as:

K-means-based Segmentation

Input: Enhanced Data of MRI → EMRI

Output: Background and Foreground of MRI in terms of ROT → B-MRI and ROT

1. Start K-means-based Segmentation
2. Initialize a group for segmentation ($G = 2$)
3. EMRI Size = [Row, Col, Plane]
4. A predetermined number of clusters, $C = C1$ and $C2$ // Where $C1$ for B-MRI and $C2$ for ROT
5. ITR = N is set for iterations.
6. While $ITR \neq N$ (if maximum iteration is not achieved) do
 For m according to Row do
 For n according to Col do
 If $EMRI[m, n] == C1$ then
 B-MRI[m, n] = EMRI[m, n]
 Else Default == $C2$
 ROT[m, n] = EMRI[m, n]
 End – If
 End – For
 End – For
7. Adjust Centroid C using their mean

$$C = \frac{\sum_{m=1}^{Row} \sum_{n=1}^{Col} (C1_{mn} + C2_{mn})}{2}$$
8. End – While
9. Return: B-MRI and ROT as a segmented MRI background and foreground
10. End – Algorithm

The K-means algorithm in the article produced better segmented results than the FCM-based model.

FCM with PSO-based ROT Segmentation: This situation works like FCM, however we employed PSO as a hybrid segmentation algorithm. PSO is the basic Meta heuristic swarm-based strategy that uses fitness to tackle segmentation mix-up. PSO was developed by Eberhart and Kennedy for evolutionary picture segmentation. The algorithm can traverse over the search space and track coordinates with fitness solution to solve unsupervised FCM clustering to improve MRI image segmentation. The FCM method utilising PSO-based ROT segmentation is stated as follows:

FCM with PSO-based Segmentation

Input: Enhanced Data of MRI → EMRI

Output: Background and Foreground of MRI in terms of ROT → B-MRI and ROT

1. Start FCM with PSO-based Segmentation

2. Size in terms of $T = \text{Size}(\text{EMRI})$

3. Define Fitness function:

$$fit(fun) = \begin{cases} 1 & \text{if pixel is less than threshold} \\ 0 & \text{otherwise} \end{cases}$$

4. For l according to T do

$fs = EMRI(l)$

$ft = \frac{\sum_{i=1}^{\text{Pixels}} EMRI(i)}{\text{Length of EMRI Pixels}}$

$fit(fun) = A/c$ to equation

$T_{value} = PSO(P, T, LB, UB, N, fit(fun))$

Where, Lower Bound (LB), Upper Bound (UB), Number of selections (N)

End – For

5. Set OITR = N // optimization iterations

6. While OITR \neq N (if not reached max iteration) do

Threshold = Threshold_value

Mask Image = Binary(ROT, Threshold)

Boundaries = Find out boundary(Mask Image)

ROT = Boundaries

For k according to D do

$ROT = EMRI \times ROT$

End – For

End – While

7. Return: B-MRI and ROT as a segmented MRI background and foreground

8. End – Algorithm

Better segmented results were obtained using the hybrid segmentation algorithm in the suggested model, which combines FCM and PSO [44], than using only FCM in the ROT segmentation model.

K-means with PSO-based ROT Segmentation: This scenario works like K-means, however we applied PSO to hybridise K-means for segmentation and the algorithm of K-means with PSO-based ROT segmentation is written as:

K-means with PSO-based Segmentation

Input: Enhanced Data of MRI → EMRI

Output: Background and Foreground of MRI in terms of ROT → B-MRI and ROT

1. Start K-means + PSO-based Segmentation

2. Size in terms of $T = \text{Size}(\text{EMRI})$

3. Define Fitness function:

$$fit(fun) = \begin{cases} 1 & \text{if pixel is less than threshold} \\ 0 & \text{otherwise} \end{cases}$$

4. For l according to T do

$fs = EMRI(l)$

$ft = \frac{\sum_{i=1}^{\text{Pixels}} EMRI(l)}{\text{Length of EMRI Pixels}}$

$fit(fun) = A/c$ to equation

$T_{value} = PSO(P, T, LB, UB, N, fit(fun))$

Where, Lower Bound (LB), Upper Bound (UB), Number of selections (N)

End – For

5. Set OITR = N // optimization iterations

6. While OITR \neq N (if not reached max iteration) do

Threshold = Threshold_value

Mask Image = Binary(ROT, Threshold)

Boundaries = Find out boundary(Mask Image)

ROT = Boundaries

For k according to D do

$ROT = EMRI \times ROT$

End – For

End – While

7. Return: B-MRI and ROT as a segmented MRI background and foreground

8. End – Algorithm

Better segmented results were obtained by the hybrid segmentation approach in the suggested system, which combined K-means with PSO, than by either the FCM with PSO-based ROT segmentation model or solely K-means-based ROT segmentation.

FCM with MFO-based ROT Segmentation: Because we compare brain tumour segmentation methods, we employed FCM with MFO as an optimization algorithm instead of PSO to build a hybrid MRI data segmentation strategy. Scalability and flexibility for MFO is better to PSO with maximum convergence speed (How quickly reach to an optimal or near-optimal solution). MFO with an optimal and innovative fitness function solve the FCM separation or pixel mix up problem during the ROT segmentation. MFO is a swarm-based bio-inspired metaheuristic algorithm inspired by moth (insect) behaviour that searches for pixels that mix together during segmentation and separates those pixels using morphological operations [45]. The algorithm of FCM with MFO-based ROT segmentation in ASBT system is written as:

FCM with MFO-based Segmentation

Input: Enhanced Data of MRI → EMRI

Output: Background and Foreground of MRI in terms of ROT → B-MRI and ROT

1. Start FCM + MFO-based Segmentation
2. Apply K-means segmentation on EMRI
3. To optimize the ROT, MFO is used on FCM output
4. Set up basic parameters of MFO: Population of Moth (PM) – Pixel count in EMRI
5. Define position function:

$$\nu(r) = \nu_0 \times \exp(-\text{distance}^m), \quad \text{if } m \geq 1$$

Where: - distance = distance between moth and light using distance formula [47]

6. ν_0 = initial velocity at $d = 0$ - m = Position of Moth (PM)

7. Define novel Fitness Function:

$$\text{fun}(\text{fit}) = \begin{cases} 1 & \text{if EMRI}_{\text{Pixel}} < \text{Threshold Pixel} \\ 0 & \text{otherwise} \end{cases}$$

8. Set ROT and B-MRI = []

9. For each m according to Row:

For each n according to Col:

CM = EMRI(m , n)

MG = $\frac{\sum_{i=1}^m \sum_{j=1}^n \text{EMRI}(m,n)}{m \times n}$

Threshold = MFO($\text{fun}(\text{fit})$, C_M , M_M)

End For

End For

10. If EMRI (Pixels) > Threshold then

ROT = EMRI

Else

B-MRI = EMRI

End If

11. Set OITR = N // optimization iterations

12. While OITR \neq N:

Mask Image = Binary(ROT, Threshold)

Boundaries = Find out boundary(Mask Image)

ROT = Boundaries

For each k according to D :

ROT = EMRI \times ROI

End For

End While

13. Return: B-MRI and ROT as segmented MRI background and foreground

14. End – Algorithm

With the help of above-mentioned hybrid segmentation algorithm using FCM with MFO-based ROT segmentation, we achieve better results but the combination with K-means is outperform that is shown in next section of article.

K-means with MFO-based ROT Segmentation: This is the last scenario of proposed comparative system and we used K-means with MFO as a hybrid segmentation technique with a novel fitness function define in the equation 8. The algorithm of K-means with MFO-based ROT segmentation is similar to the Algorithm 6, here we only used the K-means output instead of FCM output. Fig. 5 displays the segmented result alongside the original pictures, obtained using the aforementioned suggested hybrid algorithm that combines K-means with MFO as an optimization strategy. This method outperforms other cases when it comes to accurately segmenting the tumor region from MRI scans. Last but not least, the simulation compares the six scenarios described in the study article with respect to the following performance metrics: Accuracy, Sen-

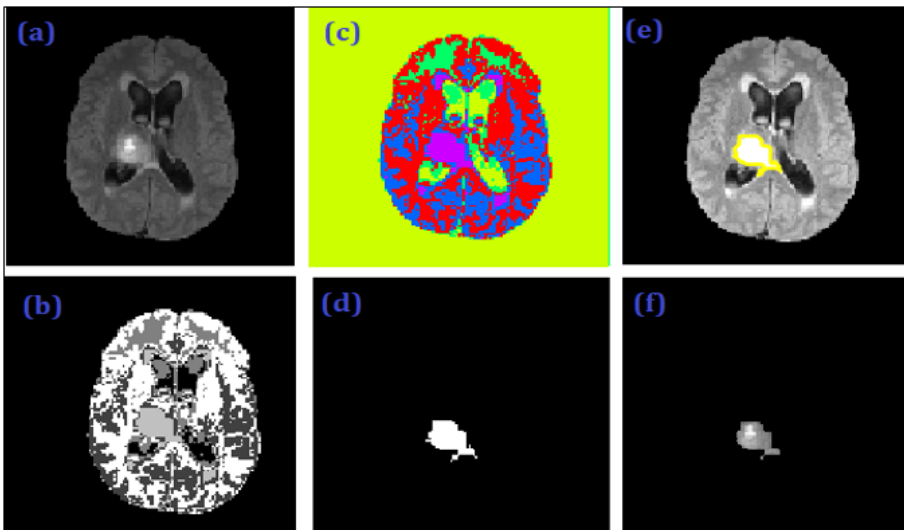


Figure 5. (a) Original MRI (b) Grey (c) Color (d) Mask Image of ROT (e) Segmented ROT Mask and (f) Segmented ROT using K-means with MFO with Maximum Accuracy

sitivity, F-measure, Precision, MCC, Dice, Jaccard, Specificity, and Time Complexity. In order to evaluate the efficacy of segmentation algorithms in precisely outlining tumor locations, it is essential to evaluate parameters during brain tumor segmentation. There is a distinct function for each of the aforementioned parameters in assessing various parts of the segmentation outcomes. The findings of the experiment and the segmentation of brain tumours utilizing the aforementioned hybrid segmentation approach are detailed in the following portion of this research article using a few sample MRI images. Fig. 6 displays the list of sample MRI images that were used from the MRI Benchmark Dataset. The dataset comprises a comprehensive collection of 3064 brain MRI slices, obtained from two distinct hospitals in China: Nanfang Hospital and General Hospital, Tianjin. The scans were gathered between 2005 and 2010. This dataset comprises three distinct types of brain tumours, namely meningioma, glioma, and pituitary tumour. The collection has a total of 708, 1426, and 930 photos for each corresponding tumour type. Essentially, meningioma and glioma are classified as malignant or cancerous, while pituitary tumours are considered benign or non-cancerous. A total of 233 individuals underwent MRI scans, resulting in the acquisition of 1025 sagittal pictures, 994 axial images, and 1045 coronal images. Our hope is that by comparing previous studies on ROT segmentation from MRI,

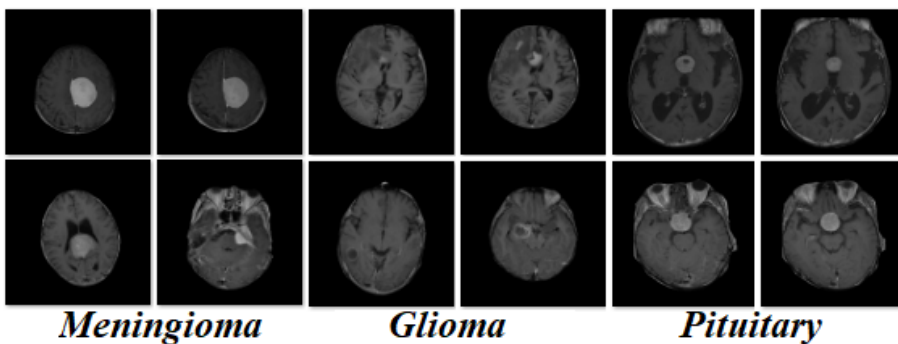


Figure 6. Sample of Brain MRI Images with Types from Dataset

we can improve our methods and ultimately get better results when analysing various proposed approaches. Table 1, which includes the source images, describes the simulation results of the suggested comparative models and its help to understand the effects of optimization approaches. The suggested comparison model of brain tumour segmentation employing the hybridization of traditional segmentation approaches with the swarm-based meta heuristic algorithms was tested

on the aforementioned dataset of sample MRI images. This study continues with a section displaying the outcomes of the suggested model’s simulations.

Model	Original MRI Images	Pre-processed MRI Images	Segmented Images			
			Labelled	Mask	Region	Tumour
1						
2						
3						
4						
5						
6						

3 Experimental Results

Using six distinct scenarios—1. FCM-based, 2. K-means-based, 3. FCM with PSO-based, 4. K-means with PSO-based, 5. FCM with MFO-based, 6. K-means with MFO-based segmentation models, we presented a comparative system for brain tumor segmentation from MRI images in this study to find out the better segmentation mechanism that will help to classify the further tumour types (Normal or Abnormal). Here, we detail the experimental outcomes of brain tumor segmentation from MRI images for 1000 test images as a sample and compare them to previous work. When compared to other methods, the segmented ROT for brain tumours produced by combining K-means and MFO performs significantly better on all test MRI images. With its more accurately delineated ROT in the segmented image (6th Row in Table 1), it is concluded to be the best of the six brain tumor segmentation procedures. In this section, we compare the segmentation results of the six different segmentation scenarios based on the performance parameters in below Table 2. Segmentation parameters are estimated and evaluated for model efficiency using Accuracy, Sensitivity, F-measure, Precision, MCC, Dice, Jaccard, Specificity, and Time Complexity. Based this comparison, we will find out better method of ROT segmentation from MRI that will help is classification task.

Based on Table 2, it is clear that K-Means with MFO optimization outperforms all other segmentation algorithms in terms of parameters like Accuracy, Sensitivity, F-measure, Precision, Matthews Correlation Coefficient (MCC), Dice coefficient, Jaccard, Specificity, and Time Complexity. Figure 7 represents the model accuracies comparison with respect to the number of simulations or tests.

Above Figure 7 represents the achieved accuracies by the different model to segment the exact ROT from the MRI data. From the figure, it is clearly seen that the accuracy of K-means with MFO-based model is far better than others and the average accuracy is 99.6% for the segmen-

Table 2. Efficiency Comparison of Proposed Comparative System

Images	FCM	K-Means	FCM+PSO	K-Means+PSO	FCM+MFO	K-Means+MFO
Accuracy						
100	90.77	94.01	95.39	96.96	98.43	99.87
200	91.22	94.86	94.95	96.46	98.08	99.56
400	90.05	92.66	95.14	96.71	97.43	99.58
500	90.32	93.11	95.08	95.86	97.33	99.73
1000	91.41	92.32	95.50	96.63	96.78	99.28
Sensitivity						
100	0.9614	0.9622	0.9703	0.9727	0.9852	0.9937
200	0.9616	0.9702	0.9761	0.9843	0.9724	0.9926
400	0.9608	0.9688	0.9707	0.9654	0.9871	0.9965
500	0.9685	0.9760	0.9856	0.9862	0.9899	0.9942
1000	0.9649	0.9653	0.9658	0.9673	0.9676	0.9815
F-measure						
100	0.1927	0.3052	0.5998	0.7082	0.8093	0.8345
200	0.2162	0.5915	0.6353	0.6572	0.8433	0.8655
400	0.2314	0.3151	0.5713	0.6102	0.6383	0.7447
500	0.3486	0.3923	0.4982	0.6708	0.7852	0.7927
1000	0.4347	0.7822	0.8779	0.9331	0.9564	0.9569
Precision						
100	0.1071	0.1814	0.4341	0.5569	0.6867	0.7194
200	0.1218	0.4255	0.4709	0.4933	0.7446	0.7674
400	0.1316	0.1882	0.4048	0.4461	0.4717	0.5945
500	0.2126	0.2455	0.3334	0.5083	0.6507	0.6582
1000	0.3506	0.4573	0.6047	0.9013	0.9455	0.9789
MCC (Matthews Correlation Coefficient)						
100	0.4526	0.4557	0.4692	0.5639	0.6052	0.8273
200	0.3962	0.5133	0.8292	0.9085	0.9529	0.9969
400	0.3061	0.3434	0.5178	0.5272	0.6472	0.9181
500	0.5564	0.6935	0.7396	0.7804	0.8480	0.8489
1000	0.5398	0.5504	0.5634	0.6121	0.6586	0.9393
Dice Coefficient						
100	0.2610	0.4461	0.5435	0.6784	0.7783	0.7810
200	0.3458	0.5126	0.5130	0.5631	0.6655	0.9714
400	0.3106	0.4694	0.4896	0.6785	0.7177	0.7809
500	0.7382	0.7944	0.8202	0.8559	0.8897	0.9194
1000	0.3392	0.4129	0.5522	0.5543	0.9745	0.9962
Jaccard						
100	0.2137	0.5091	0.6243	0.8404	0.8455	0.8968
200	0.4874	0.5388	0.7795	0.8184	0.8516	0.9099
400	0.2123	0.3325	0.4977	0.6438	0.6984	0.7602
500	0.2323	0.3467	0.8579	0.8665	0.8802	0.9166
1000	0.1016	0.1993	0.3016	0.3529	0.8555	0.9099
Specificity						
100	0.9116	0.9291	0.9324	0.9555	0.9682	0.9736
200	0.9121	0.9222	0.9433	0.9715	0.9779	0.9968
400	0.9261	0.9356	0.9389	0.9774	0.9803	0.9998
500	0.9370	0.9399	0.9449	0.9549	0.9838	0.9907
1000	0.9139	0.9337	0.9438	0.9515	0.9615	0.9765
Time Complexity (s)						
100	1.257	3.129	4.705	2.733	1.275	0.879
200	1.875	2.502	3.007	2.717	1.822	0.848
400	1.032	2.241	2.407	2.712	2.674	0.934
500	2.484	2.833	2.837	1.166	2.688	0.744
1000	1.497	2.991	4.656	3.864	1.955	1.103

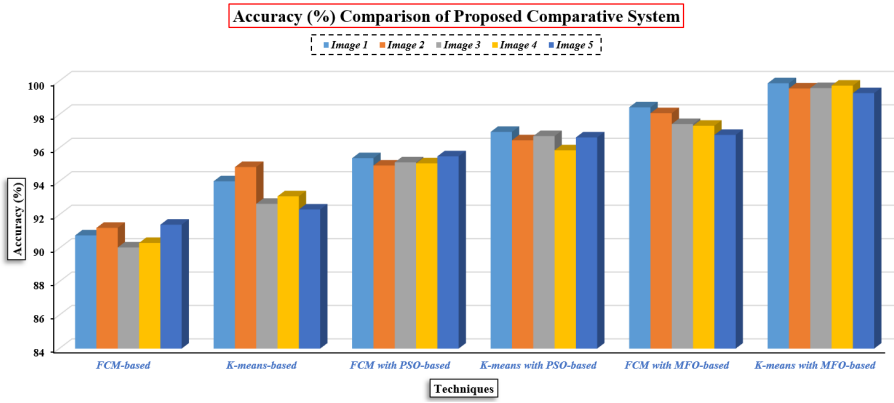


Figure 7. Accuracy (%) Comparison of Proposed Comparative System

tation based on their ground truth data. The accuracy of a model is a measure of how well the model’s segmentation match the actual outcomes or ground truth in the dataset. While accuracy is a significant indicator, it is not the sole aspect that defines the total efficiency or efficacy of a model. So, here we also calculate Precision, Recall (Sensitivity), F-measure and Time Complexity that is shown in the Figure 8.

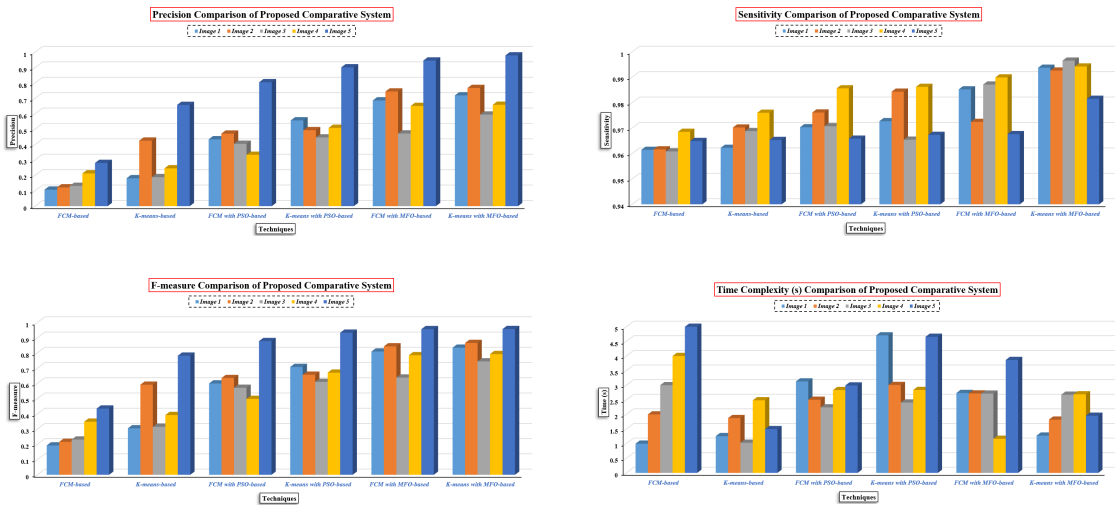


Figure 8. Precision, Recall, F-measure, and Time Complexity Comparison of Proposed Comparative System

An essential notion in algorithm analysis is shown in the Figure 8 with four different parameters named as precision, recall, f-measure and time complexity. Here, time complexity measures how long it takes for an algorithm to process an input in relation to its size. It explains, theoretically speaking, how the running time of the algorithm grows with the size of the input. From the figure, it is clear that the model with K-means with MFO-based segmentation outperform than other in terms of all parameters with time complexity. Here, computational time is slightly higher than others, but model efficiency is far better than other approaches. The proposed comparative model is also compared to other works which are previously proposed on brain tumor segmentation using MRI images. Table 3 describes these other works that are considered in this research article’s survey. We draw a comparison graph of the proposed model with existing works based on the observed values. The models used in these works use different approaches and algorithms for ROT segmentation.

Table 3. Contrast with Already Existing Works

Accuracy (%)	Authors/Techniques
97.5	MS Alam et al. [25]
97.7	A Boussselham et al. [26]
90.7	FCM-based Model [16]
93.3	K-means-based Model [14]
95.2	FCM with PSO-based Model [25]
96.5	K-means with PSO-based Model [15],[18]
97.6	FCM with MFO-based Model [26]
99.6	K-means with MFO-based Model

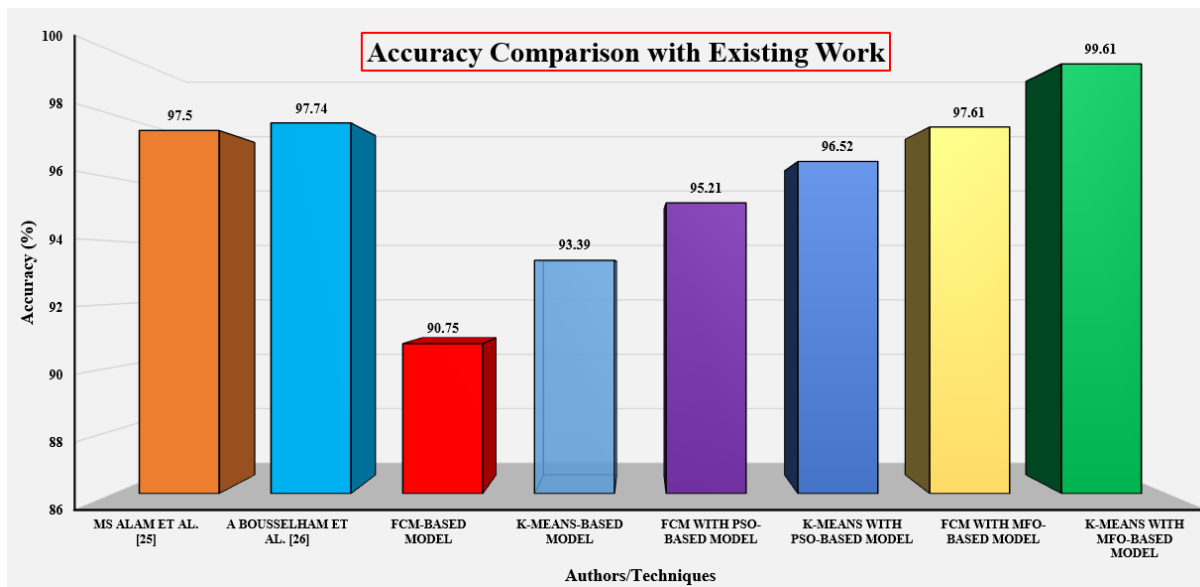
**Figure 9.** Models Comparison with Existing Work

Figure 9 presents a comparison of the planned comparative models with six distinct approaches to the work that has already been done that is now available. We can see from the graph that the suggested system, which makes use of the hybridization of K-means with MFO for ROT segmentation, obtains a higher level of accuracy than other methods or the work of other authors when it comes to the segmentation of the tumor region from the MRI image. Through the utilization of the hybrid segmentation strategy that combines K-means and MFO as an optimization approach, we are able to reach a segmentation accuracy of over 99%. Furthermore, we are able to assert that the suggested system with K-means and MFO is more effective than other methodologies and could be used in the brain tumor classification task with deep learning models.

4 Conclusion and Future Work

In this paper, we present a comparative scenario to find out the better hybridization approach for tumor region segmentation from the MRI images and we propose six different models named FCM-based, K-means-based, FCM with PSO-based, K-means with PSO-based, FCM with MFO-based, K-means with MFO-based segmentation. Basically, we try to find out better approach of segmentation for MRI images using the concept of improvisation of traditional clustering mechanisms in this paper, and to test the model efficiency, the famous and publicly available MRI benchmark dataset is used that contains multiple MRI images of human brain in the form of DICOM but we convert the into JPG format. Various ROT segmentation algorithms are compared based on accuracy, sensitivity, F-measure, precision, mcc, dice, Jaccard, specificity, and time complexity, as clearly shown in the results section of the article, where the combination of K-means with MFO-based segmentation outperforms others in all aspects. Additionally, the best model is compared with different state-of-the-art models to validate model efficiency, and the suggested model's segmentation accuracy exceeds 99.6% when simulated using MRI images, while the accuracy of the existing non-hybrid model is significantly lower. In the future, the proposed comparative system has the potential to be expanded for big MRI image datasets that consist of over one million MRI images with their classification to detect tumours in early stages. This extension would also include the ability to handle low contrast images as well as noisy images, as the system's accuracy currently declines when processing such MRI images.

References

- [1] Bhatt, C., Kumar, I., Vijayakumar, V., Singh, K. U., & Kumar, A. (2020). The state of the art of deep learning models in medical science and their challenges. *Multimedia Systems*, 1-15.
- [2] Tiwari, A., Srivastava, S., & Pant, M. (2020). Brain tumor segmentation and classification from magnetic resonance images: Review of selected methods from 2014 to 2019. *Pattern Recognition Letters*, 131, 244-260.
- [3] Bengio, Y., Courville, A. C., & Vincent, P. (2012). Unsupervised feature learning and deep learning: A review and new perspectives. *CoRR*, abs/1206.5538, 1, 2012.
- [4] Cetin, O., Seymen, V., & Sakoglu, U. (2020). Multiple sclerosis lesion detection in multimodal MRI using simple clustering-based segmentation and classification. *Informatics in Medicine Unlocked*, 20, 100409.
- [5] Raja, P. S. (2020). Brain tumor classification using a hybrid deep autoencoder with Bayesian fuzzy clustering-based segmentation approach. *Biocybernetics and Biomedical Engineering*, 40(1), 440-453.
- [6] Bonabeau, E., Marco, D. D. R. D. F., Dorigo, M., Théraulaz, G., & Theraulaz, G. (1999). *Swarm intelligence: from natural to artificial systems* (No. 1). Oxford university press.
- [7] Banks, A., Vincent, J., & Anyakoha, C. (2007). A review of particle swarm optimization. Part I: background and development. *Natural Computing*, 6(4), 467-484.
- [8] Kennedy, J., & Eberhart, R. (1995, November). Particle swarm optimization. In *Proceedings of ICNN'95-international conference on neural networks* (Vol. 4, pp. 1942-1948). IEEE.
- [9] Karaboğa, D. (2005). *An Idea Based on Honey Bee Swarm for Numerical Optimization*.
- [10] Yang, X. S. (2009, October). Firefly algorithms for multimodal optimization. In *International symposium on stochastic algorithms* (pp. 169-178). Springer, Berlin, Heidelberg.
- [11] Yang, X. S., & Deb, S. (2009, December). Cuckoo search via Lévy flights. In *2009 World congress on nature & biologically inspired computing (NaBIC)* (pp. 210-214). IEEE.

- [12] Saremi, S., Mirjalili, S., & Lewis, A. (2017). Grasshopper optimisation algorithm: theory and application. *Advances in Engineering Software*, 105, 30-47.
- [13] Chander, A., Chatterjee, A., & Siarry, P. (2011). A new social and momentum component adaptive PSO algorithm for image segmentation. *Expert Systems with Applications*, 38(5), 4998-5004.
- [14] Bandhyopadhyay, S. K., & Paul, T. U. (2013). Automatic segmentation of brain tumour from multiple images of brain MRI. *Int J Appl Innovat Eng Manage (IJAIEM)*, 2(1), 240-248.
- [15] Zhao, M., Tang, H., Guo, J., & Sun, Y. (2014). Data clustering using particle swarm optimization. In *Future information technology* (pp. 607-612). Springer, Berlin, Heidelberg.
- [16] Jose, A., Ravi, S., & Sambath, M. (2014). Brain tumor segmentation using k-means clustering and fuzzy c-means algorithms and its area calculation. *International Journal of Innovative Research in Computer and Communication Engineering*, 2(3).
- [17] Parasar, D., & Rathod, V. R. (2017). Particle swarm optimisation K-means clustering segmentation of foetus ultrasound image. *International Journal of Signal and Imaging Systems Engineering*, 10(1-2), 95-103.
- [18] Venkatesan, A., & Parthiban, L. (2017). Medical Image Segmentation with Fuzzy C-Means and Kernelized Fuzzy C-Means Hybridized on PSO and QPSO. *International Arab Journal of Information Technology (IAJIT)*, 14(1).
- [19] Hasan, A. M. (2018). A hybrid approach of using particle swarm optimization and volumetric active contour without edge for segmenting brain tumors in MRI scan. *Indonesian Journal of Electrical Engineering and Informatics (IJEI)*, 6(3), 292-300.
- [20] Karegowda, A. G., Poornima, D., Sindhu, N., & Bharathi, P. T. (2018). Performance Assessment of k-Means, FCM, ARKFCM and PSO Segmentation Algorithms for MR Brain Tumour Images. *International Journal of Data Mining and Emerging Technologies*, 8(1), 18-26.
- [21] Arunkumar, N., Mohammed, M. A., Abd Ghani, M. K., Ibrahim, D. A., Abdulhay, E., Ramirez-Gonzalez, G., & de Albuquerque, V. H. C. (2019). K-means clustering and neural network for object detecting and identifying abnormality of brain tumor. *Soft Computing*, 23(19), 9083-9096.
- [22] Hrosik, R. C., Tuba, E., Dolicanin, E., Jovanovic, R., & Tuba, M. (2019). Brain image segmentation based on firefly algorithm combined with k-means clustering. *Stud. Inform. Control*, 28, 167-176.
- [23] Chander, P. S., Soundarya, J., & Priyadharsini, R. (2020). Brain Tumour Detection and Classification Using K-Means Clustering and SVM Classifier. In *RITA 2018* (pp. 49-63). Springer, Singapore.
- [24] Magadza, T., & Viriri, S. (2021). Deep learning for brain tumor segmentation: a survey of state-of-the-art. *Journal of Imaging*, 7(2), 19.
- [25] Hanuman Verma, Deepa Verma, Pawan Kumar Tiwari (2021). A population based hybrid FCM-PSO algorithm for clustering analysis and segmentation of brain image. *Expert Systems with Applications*, Volume 167, 114121.
- [26] K. Anita Davamani, C.R. Rene Robin, D. Doreen Robin, L. Jani Anbarasi (2022). Adaptive blood cell segmentation and hybrid Learning-based blood cell classification: A Meta-heuristic-based model. *Biomedical Signal Processing and Control*, Volume 75, 103570.
- [27] Alam, M. S., Rahman, M. M., Hossain, M. A., Islam, M. K., Ahmed, K. M., Ahmed, K. T., & Miah, M. S. (2019). Automatic Human Brain Tumor Detection in MRI Image Using Template-Based K Means and Improved Fuzzy C Means Clustering Algorithm. *Big Data and Cognitive Computing*, 3(2), 27.
- [28] Bousselham, A., Bouattane, O., Youssfi, M., & Raihani, A. (2019). Towards reinforced brain tumor segmentation on MRI images based on temperature changes on pathologic area. *International journal of biomedical imaging*, 2019.
- [29] Yuan, Y., Chao, M., & Lo, Y. C. (2017). Automatic skin lesion segmentation using deep fully convolutional networks with jaccard distance. *IEEE transactions on medical imaging*, 36(9), 1876-1886.
- [30] Riaz, F., Naeem, S., Nawaz, R., & Coimbra, M. (2018). Active contours-based segmentation and lesion periphery analysis for characterization of skin lesions in dermoscopy images. *IEEE Journal of Biomedical and Health Informatics*, 23(2), 489-500.
- [31] Vasconcelos, F. F. X., Medeiros, A. G., Peixoto, S. A., & Reboucas Filho, P. P. (2019). Automatic skin lesions segmentation based on a new morphological approach via geodesic active contour. *Cognitive Systems Research*, 55, 44-59.
- [32] Siegel, R. L., Miller, K. D., & Jemal, A. (2019). Cancer statistics, 2019. *CA: A Cancer Journal for Clinicians*, 69(1), 7-34.
- [33] O'Sullivan, D. E., Brenner, D. R., Demers, P. A., Villeneuve, P. J., Friedenreich, C. M., King, W. D., & ComPARE Study Group. (2019). Indoor tanning and skin cancer in Canada: A meta-analysis and attributable burden estimation. *Cancer Epidemiology*, 59, 1-7.
- [34] Wei, Z., Song, H., Chen, L., Li, Q., & Han, G. (2019). Attention-Based DenseUnet Network with Adversarial Training for Skin Lesion Segmentation. *IEEE Access*, 7, 136616-136629.

- [35] Tan, T. Y., Zhang, L., Lim, C. P., Fielding, B., Yu, Y., & Anderson, E. (2019). Evolving ensemble models for image segmentation using enhanced particle swarm optimization. *IEEE Access*, 7, 34004-34019.
- [36] Xie, F., Yang, J., Liu, J., Jiang, Z., Zheng, Y., & Wang, Y. (2020). Skin lesion segmentation using high-resolution convolutional neural network. *Computer Methods and Programs in Biomedicine*, 186, 105241.
- [37] Zhang, C., Xiao, X., Li, X., Chen, Y. J., Zhen, W., Chang, J., & Liu, Z. (2014). White blood cell segmentation by color-space-based k-means clustering. *Sensors*, 14(9), 16128-16147.
- [38] Mondal, P. K., Prodhon, U. K., Al Mamun, M. S., Rahim, M. A., & Hossain, K. K. (2014). Segmentation of white blood cells using fuzzy C means segmentation algorithm. *IOSR Journal of Computer Engineering*, 1(16), 1-5.
- [39] Madhloom, H. T., Kareem, S. A., & Ariffin, H. (2015). Computer-aided acute leukemia blast cells segmentation in peripheral blood images. *Journal of Vibroengineering*, 17(8), 4517-4532.
- [40] Su, J., Liu, S., & Song, J. (2017). A segmentation method based on HMRF for the aided diagnosis of acute myeloid leukemia. *Computer Methods and Programs in Biomedicine*, 152, 115-123.
- [41] ElDahshan, K., Youssef, M., Masameer, E., & Mustafa, M. A. (2015). An efficient implementation of acute lymphoblastic leukemia images segmentation on the FPGA. *European Journal of Applied Sciences*, 3(3), 8-8.
- [42] Dhal, K. G., Gálvez, J., Ray, S., Das, A., & Das, S. (2020). Acute lymphoblastic leukemia image segmentation driven by stochastic fractal search. *Multimedia Tools and Applications*, 1-29.
- [43] Kumar, S., & Aggarwal, A. (2023, November). Gene Expression based Blood Cancer Classification Model using Natural Computing along with Deep Learning. In *2023 International Conference on Communication, Security and Artificial Intelligence (ICCSAI)* (pp. 292-297). IEEE.
- [44] Aggarwal, N., & Kumar, S. (2024, July). An Optimized TF-IDF Features based Deep Learning Enabled Automated Fake News Detection Scheme. In *2024 Asia Pacific Conference on Innovation in Technology (APCIT)* (pp. 1-9). IEEE.
- [45] Shinde, S. S., Macha, J., & Ramane, H. S. (2024). Bounds for Sombor Eigenvalue and Energy of a Graph in Terms of Hyper Zagreb and Zagreb Indices. *Palestine Journal of Mathematics*, 13(1).
- [46] Ekhad, S. B., & Zeilberger, D. (2022). Invariance Properties of Matrix Powers. *Palestine Journal of Mathematics*, 11(1), 1-5.
- [47] Mehdi-Nezhad, E., & Rahimi, A. M. (2022). Substructures with an Almost Division Algorithm in Euclidean Commutator Lattices. *Palestine Journal of Mathematics*, 11(1).

Author information

Mohit Prakram, Department of Computer Science and Engineering, Lovely Professional University, Phagwara, India.

E-mail: mohit.15284@lpu.co.in

Kirti Rawal, Department of Electronics and Communication, Lovely Professional University, Phagwara, India.

E-mail: kirti.20248@lpu.co.in

Manu Prakram, Department of Electronics and Communication, Lovely Professional University, Phagwara, India.

E-mail: manu.14704@lpu.co.in

Parul Sharma, Department of Computer Science and Engineering, Lovely Professional University, Phagwara, India.

E-mail: parul.16466@lpu.co.in